



Sea level rise drowned a vast habitable area of north-western Australia driving long-term cultural change

Kasih Norman^{a,b,c,*}, Corey J.A. Bradshaw^{c,d}, Frédérik Saltré^{c,d}, Chris Clarkson^{e,f,b,c},
Tim J. Cohen^c, Peter Hiscock^{e,g}, Tristen Jones^{h,c}, Fabian Boesl^c

^a Australian Research Centre for Human Evolution, Griffith University, Queensland, 4222, Australia

^b Centre for Archaeological Science, School of Earth, Atmospheric and Life Sciences, University of Wollongong, Wollongong, New South Wales 2522, Australia

^c ARC Centre of Excellence for Australian Biodiversity and Heritage, University of Wollongong, Wollongong, New South Wales, Australia

^d Global Ecology | Partuyarta Ngadluku Wardli Kuu, College of Science and Engineering, Flinders University, GPO Box 2100, Adelaide, South Australia 5001, Australia

^e School of Social Science, University of Queensland, St Lucia, Queensland 4072, Australia

^f Department of Archaeology, Max Planck Institute for the Science of Human History, Kahlaische Strasse 10, Jena 07745, Germany

^g Faculty of Science, Medicine and Health, University of Wollongong, New South Wales 2522, Australia

^h School of Humanities, Faculty of Arts and Social Science, The University of Sydney, Sydney, New South Wales 2006, Australia

ARTICLE INFO

Handling editor: I Hendy

Keywords:

Australia
Pleistocene Sahul
Human occupation
Human dispersal
Australian archaeology
Rock art
Paleogeography
Drowned landscapes
Continental shelf
Sea level change
Bathymetry

ABSTRACT

For most of the period of human occupation of Sahul (the combined Pleistocene landmass of Australia and New Guinea), lower sea levels exposed an extensive area of the northwest of the Australian continent, connecting the Kimberley and Arnhem Land into one vast area. Our analysis of high-resolution bathymetric data shows this now-drowned region existed as an extensive archipelago in Marine Isotope Stage 4, transforming in Marine Isotope Stage 2 into a fully exposed shelf containing an inland sea adjacent to a large freshwater lake. These were encircled by deep gorges and escarpments that likely acted as important resource zones and refugia for human populations at that time. Demographic modelling shows the shelf had a fluctuating potential carrying capacity through Marine Isotope Stages 4–2, with the capability to support 50–500 k people at various times. Two periods of rapid global sea level rise at 14.5–14.1 ka (Meltwater Pulse 1A), and between 12 ka and 9 ka, resulted in the rapid drowning of ~50% of the Northwest Shelf. This likely caused a retreat of human populations, registering as peaks in occupational intensity at archaeological sites. We contend that the presence of an extensive archipelago on the Northwest Shelf in Marine Isotope Stage 4 facilitated the successful dispersal of the first maritime explorers from Wallacea, creating a familiar environment for their maritime economies to adapt to the vast terrestrial continent of Sahul.

1. Introduction

Drowned archaeological sites demonstrating global human use of now-submerged continental shelves have been found in the Baltic Sea (Grøn and Skaarup, 2004), north-western Europe (Bicket and Tizzard, 2015; Gaffney et al., 2017; Tizzard et al., 2014), the Mediterranean coast (Galili et al., 1993; Sturt et al., 2018), North and South America (Bayón and Politis, 2014; López et al., 2016; Sturt et al., 2018), South Africa (Werz and Flemming, 2001), and on the Australian shelf (Benjamin et al., 2020, 2023). Aside from an early pioneering study (Flemming, 1982, 1983), Australia has traditionally lagged behind many parts of the world with respect to exploration of the archaeology of submerged continental shelves, but recently there has been a proliferation of

predictive site models (Benjamin et al., 2018; Ditchfield et al., 2022; O'Leary et al., 2020; Veth et al., 2020; Ward et al., 2015) and archaeological surveys of submerged landscapes (Benjamin et al., 2020; Leach et al., 2021; McCarthy et al., 2022; Wiseman et al., 2021).

The submerged Northwest Shelf of Sahul (the combined landmass of Australia and New Guinea at times of lower sea level) was a vast area of land in the Late Pleistocene that connected the Australian regions of the Kimberley and western Arnhem Land during times of lower sea level than today. The shelf extends >500 km northwest from the modern-day shoreline (Fig. 1) with a now-submerged landmass of ~400,000 km², an area more than 1.6 times larger than the United Kingdom. The region might have been an area of initial entry for the peopling of Sahul (Bird et al., 2018; Bradshaw et al., 2021, 2023; Kuijjer et al., 2022; Norman

* Corresponding author. Australian Research Centre for Human Evolution, Griffith University, Queensland 4222, Australia.

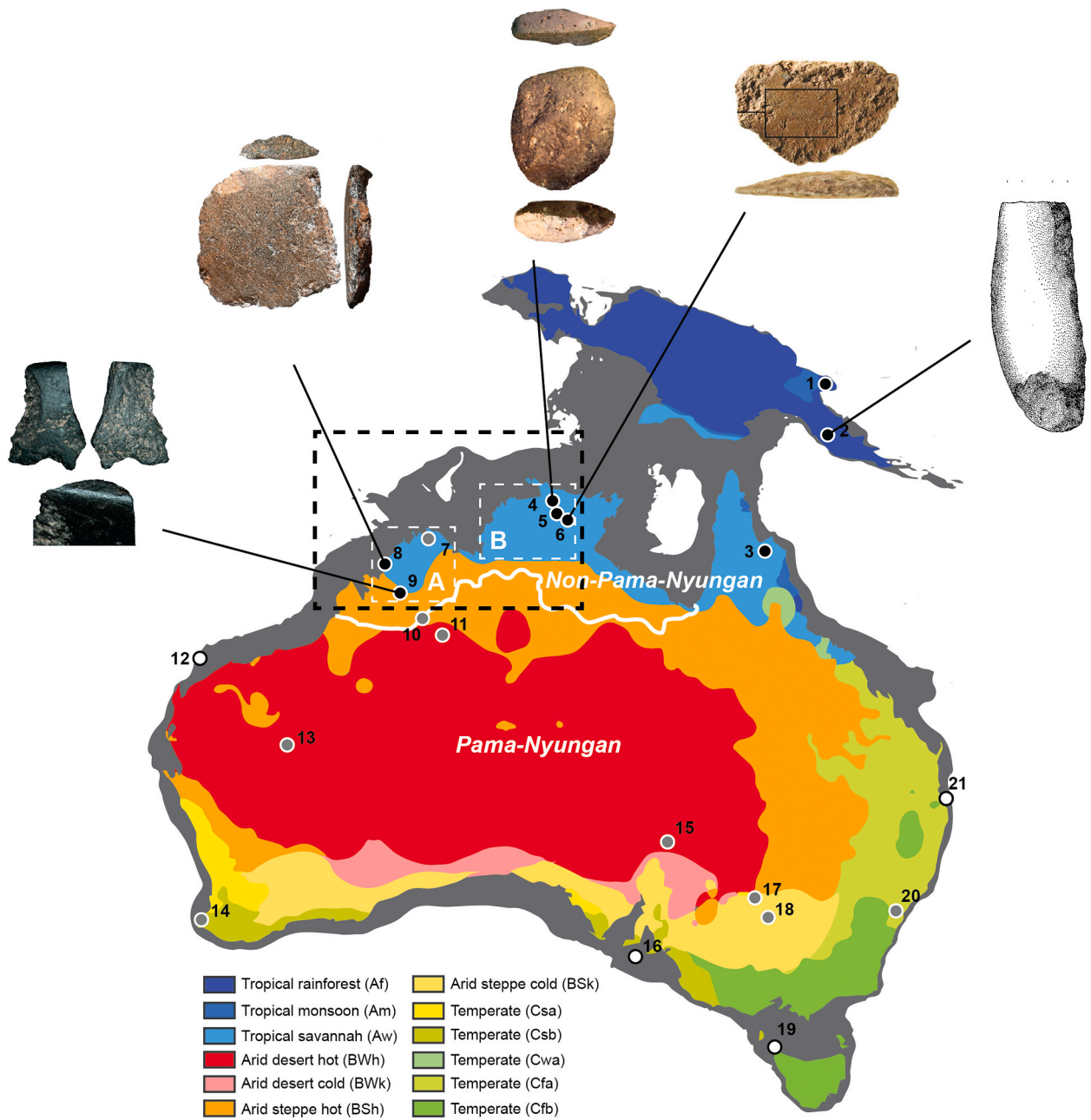
E-mail address: kasih.norman@griffith.edu.au (K. Norman).

<https://doi.org/10.1016/j.quascirev.2023.108418>

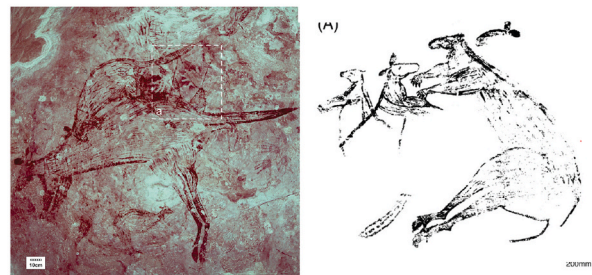
Received 13 July 2023; Received in revised form 1 November 2023; Accepted 7 November 2023

Available online 15 December 2023

0277-3791/© 2023 The Authors. Published by Elsevier Ltd. This is an open access article under the CC BY license (<http://creativecommons.org/licenses/by/4.0/>).



A Kimberley IIA style



B Arnhem Land ELNF style

(caption on next page)

Fig. 1. Map of Sahul showing the extent of the now-submerged continental shelf (dark grey), with the area of the Northwest Shelf demarcated by a dashed black box, and the present-day distribution of the Köppen climate groups (seasonal precipitation and temperature) showing the extent of modern-day Australia and New Guinea. The tropical distribution of Late Pleistocene sites containing early axe technology are shown as black circles, sites without early axe technology as grey circles, and sites demonstrating Late Pleistocene occupation of the now submerged continental shelves as white circles. Site numbers indicate 1. Bobongara, 2. Kosipe, 3. Sandy Creek, 4. Madjedbebe, 5. Nauwalabila I, 6. Nawarla Gabarnmang, 7. Minjiwarra, 8. Widingarri, 9. Carpenter's Gap 1, 10. Riwi, 11. Parnkupirti, 12. Boodie Cave, 13. Karnatukul, 14. Devil's Lair, 15. Warraty, 16. Seton Rockshelter, 17. Lake Menindee, 18. Lake Mungo, 19. Cave Bay Cave, 20. Pitt Town, 21. Wallen Wallen Creek. Dashed white boxes show the approximate location of **A** the Kimberley irregular infill animal style (image courtesy of Damien Finch) and, **B** the Arnhem Land 'early large naturalistic fauna' style (image courtesy of Tristen Jones). The approximate position of the non-Pama-Nyungan language boundary is shown by a white line. Axe images: 2. Image courtesy of Glen Summerhayes, 4. Image courtesy of Chris Clarkson, 6. Image courtesy of Bruno David, 8. Image courtesy of Ceri Shipton, 9. Image courtesy of Peter Hiscock.

et al., 2018; Sturt et al., 2018). Irrespective of the precise locations people used to disperse into Sahul, the Northwest Shelf is adjacent to the oldest known archaeological sites in Australia (Clarkson et al., 2017; Maloney et al., 2018; Norman et al., 2022; Roberts et al., 1994), and might have been one of the first inhabited landscapes on the continent (Bradshaw et al., 2021; Norman et al., 2018). Archaeological evidence for Late Pleistocene use of the continental shelves of Sahul by the First Australians is demonstrated on multiple large islands that are remnant portions of the continental margin, including Barrow Island (Veth et al., 2017), Kangaroo Island (Hope et al., 1977), Hunter Island (Bowdler, 1975), and Minjiwarra (Stradbroke Island) (Neal and Stock, 1986). Together, evidence is emerging for human use of the Australian continental shelves, but the potential of the vast submerged region stretching between the Kimberley and Arnhem Land as a Late Pleistocene cultural landscape has not been investigated.

The Northwest Shelf is dominated by the Bonaparte Basin, a large depression containing a smaller sub-basin at its centre that remained permanently connected to the open ocean by the Malita Valley (Bourget et al., 2012; Courgeon et al., 2016) (Supplementary Information, Supplementary Fig. S1-S2). Partially surrounding the Malita sub-basin are three extensive landforms consisting of flat-topped, carbonate terrace platforms that are deeply incised (Londonderry, Sahul, and Van Diemen Rises) (Supplementary Fig. S1), comparable to the plateau regions of the Kimberley and Arnhem Land (Anderson et al., 2011; Clarke and Ringis, 2000; Heap et al., 2010; Ishiwa et al., 2016a). Previous studies of the Northwest Shelf of Sahul have focused on the tectonic, geomorphic, and palaeo-environmental development of the region, commonly over geological timescales. We contend that the emergent Northwest Shelf connecting the Kimberley and Arnhem Land (Fig. 1) formed one vast cultural and biogeographic region during the Late Pleistocene. Evidence for an early shared cultural tradition across northern Sahul takes three forms: (1) Late Pleistocene axe technology found only in tropical north Australia and New Guinea from first occupation until the mid-Holocene (Clarkson et al., 2022; Golson et al., 2001; Groube, 1986; O'Connor, 1999) (Supplementary Table S1), (2) similarity in the 'early naturalistic' rock-art traditions represented by the 'irregular infill animal' style in the Kimberley and the 'early large naturalistic fauna' style in Arnhem Land (Chaloupka, 1993; Chippindale and Tacon, 1998; Finch et al., 2021; Jones et al., 2020; Lewis, 1988, 1997; Veth et al., 2018; Walsh, 1994), and (3) distinctive and highly diverse non-Pama-Nyungan language families spoken in both the Kimberley and Arnhem Land today, with the rest of Australia dominated by the relatively homogenous Pama-Nyungan language family (Clendon, 2006; Dixon, 1997; Koch, 1997) (Fig. 1).

Here, we consider the potential of the landscape features and environments of the Northwest Shelf to support a human population during the Late Pleistocene. We used high-resolution bathymetric data to reveal the environmental characteristics of the now-submerged landscapes of the Northwest Shelf in the Late Pleistocene (Marine Isotope Stages 4–2). We estimated human carrying capacity for the submerged shelf using a hindcasted Earth system model, approximating plausible human population size for Marine Isotope Stages 4–2. Finally, we show two rapid pulses in sea level rise during Meltwater Pulse 1A (14.5–14.1 ka, with ka = 1000 years) and the onset of the Holocene correspond to peaks in stone artefact discard rates at key sites in the Kimberley and Arnhem

Land, for the first time demonstrating an archaeological signature for human populations retreating off the Northwest Shelf.

2. Methods

2.1. Sea-level projections and environmental proxy data

The Australia northwest continental shelf margin represents an excellent region for the study of sea level change, remaining tectonically stable since the Marine Isotope Stage 5e sea level highstand (Yokoyama et al., 2001a). To visualise the inundation and exhumation history of the Northwest Shelf, we projected past sea levels (Ishiwa et al., 2019; Lambeck and Chappell, 2001; Williams et al., 2018) onto the high-resolution depth model for Northern Australia –30 m (Beaman, 2018) in ArcGIS Pro 3.0. Many factors can introduce error when projecting past sea levels onto bathymetric data, including the sea-level curve, with eustatic (global) and regional sea-level curves often conflicting, and even regional sea-level curves within similar geographic areas demonstrating dissimilarity (Lambeck and Chappell, 2001; Lewis et al., 2013). We used the most appropriate sea-level curve available for each Marine Isotope Stage. Because regional sea-level curves prior to Marine Isotope Stage 2 are lacking in our study area (Lewis et al., 2013), we projected the New Guinea Huon Terrace eustatic sea level curve (Lambeck and Chappell, 2001) for the Marine Isotope Stage 4 lowstand and Stage 3 highstand. Seismic survey data indicate local sea levels in the Bonaparte Basin were –80 m in Marine Isotope Stage 4, agreeing with the lower range of the Huon Terrace curve for that time (Fogg et al., 2022; Kuijper et al., 2022; Lambeck and Chappell, 2001). Marine Isotope Stage 2 is well-constrained by the Bonaparte Basin regional sea-level curve, which covers the period 28–12 ka (Ishiwa et al., 2019). We projected Holocene sea-level rise and stabilisation using a published aggregated Australian sea-level curve (Williams et al., 2018), which represents a line of best fit from an Australia-wide dataset (Lewis et al., 2013).

Projections can also be affected by vertical error within the bathymetric dataset (Beaman, 2018), the mantle rheology (glacio-hydro-isostatic ice and water loading depressing the mantle), vertical tectonic movement, and post-sea-level rise sedimentation of the ocean floor. Sea-level projections on the Northwest Shelf can be affected to some degree by hydro-isostasy, with the amplitude of this effect estimated to <20 m in the Bonaparte Basin (Ishiwa et al., 2016a, 2019; Yokoyama et al., 2001a, 2001b). Australia is one of the most tectonically stable continents, with limited isostatic influence from hydro-isostasy and no glacio-isostatic effects. This has made the northern Australia region a core area in Quaternary sea-level studies (Lambeck and Chappell, 2001; Woodroffe et al., 1986). Vertical tectonic movement due to subsidence of the north-western Australian Shelf might have affected the modern bathymetry of the region relative to past landscape values. While there are no data available for the Bonaparte Basin, there are studies to the south of the region adjacent to the Browse and Roebuck Basins, which show long-term average subsidence rates of 0.064 m/ka–0.125 m/ka, with an acceleration in the late Miocene (Belde et al., 2017). Late Pleistocene rates are in the range of 0.2 m/ka for Adele Reef and between 0.29 m/ka–0.45 m/ka for Scott Reef, suggesting stronger subsidence towards the outer shelf (Collins et al., 2011; Solihuddin et al.,

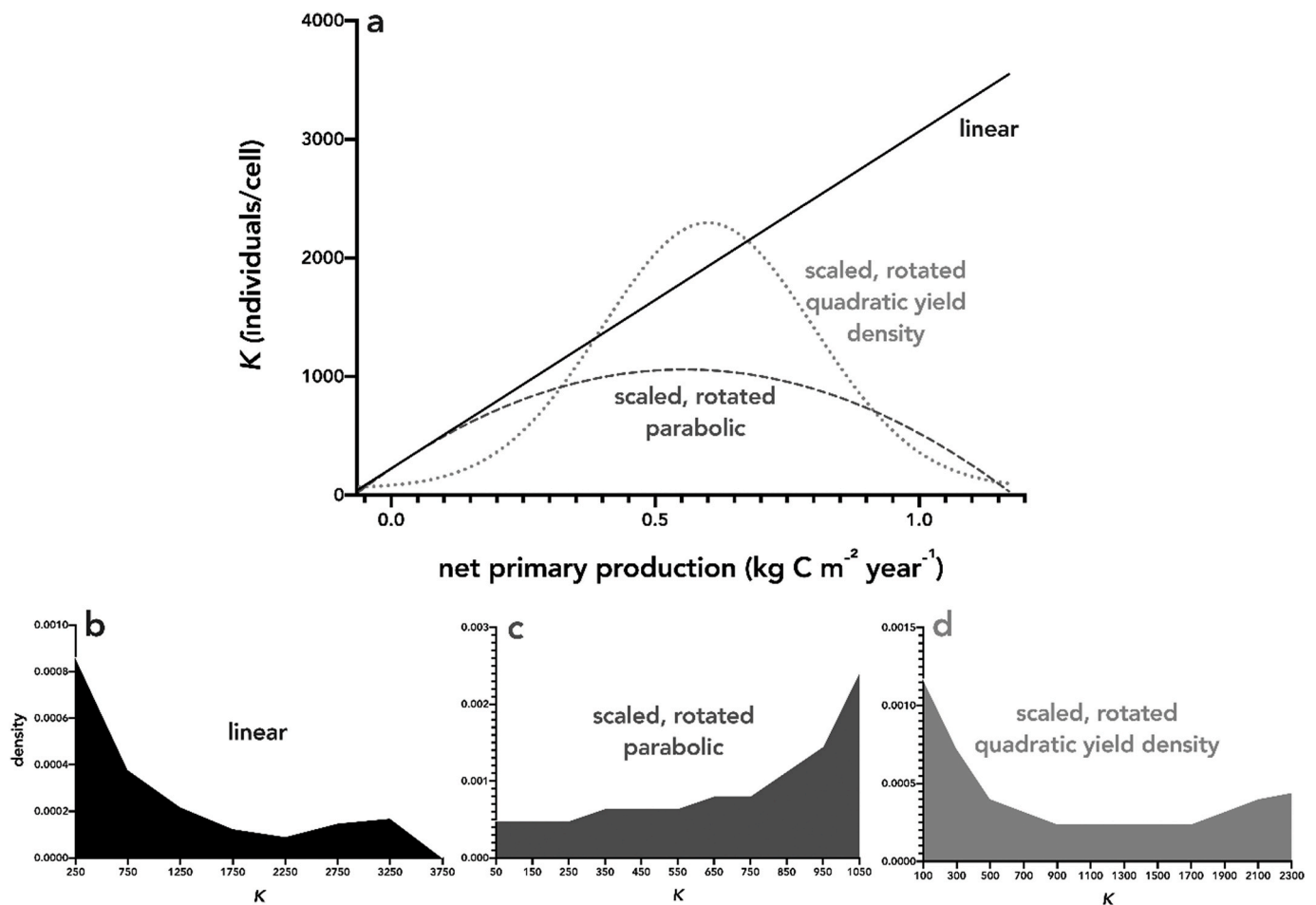


Fig. 2. (a) Relationships between net primary production and per-cell carrying capacity (K), assuming either a positive linear, rotated parabolic, or rotated quadratic yield-density relationship. The latter relationship is scaled such that K_{\max} for the rotated parabolic and quadratic yield-density relationships is $0.5K_{\max}$ of the linear relationship, and where the latter's ΣK_{\max} across all cells and temporal layers = ΣK_{\max} of the linear relationship. This is because under the linear assumption, there are fewer cells with high carrying capacity (density plot; panel b) compared to the rotated parabolic assumption (panel c), and there are more high- K cells under the quadratic yield-density assumption (panel d) compared to the linear (panel b).

2016). Sedimentation rates are low across the Bonaparte Basin. Cores show a ~ 15 -m thick wedge of Holocene sediment along the modern coastal margin (Clarke and Ringis, 2000; Collins et al., 2011), with post-glacial marine transgression sedimentation of the ocean floor thinning to 2–5 m across most of the shelf (De Deckker and Yokoyama, 2009; Ishiwa et al., 2016a,b; Yokoyama et al., 2001a).

Where possible, we validated sea-level curve projections on the Northwest Shelf bathymetric data against published environmental proxy data. Projected sea-level curves correspond well to published palaeo-environmental records (Ishiwa et al., 2019; Yokoyama et al., 2000, 2001a) from cores in the Bonaparte Basin (Supplementary Figs. S2–S3). Re-calibration (Heaton et al., 2020) of the radiocarbon age estimates (Supplementary Table S2) (using Calib Rev 8.1.0 (Stuiver and Reimer, 1993) and the Marine20 curve for shell (Heaton et al., 2020)) dating the five Malita Basin environments of open marine, shallow marine, marginal marine, intertidal, and brackish lagoonal/estuarine allowed comparison to our projections.

2.2. Drowned landscape feature identification

We projected the high-resolution depth model for Northern Australia ~ 30 m (Beaman, 2018) in ArcGIS Pro 3.0 and visually interrogated it for palaeochannels and gorge systems. We identified four regions with incised palaeochannels, and measured their lengths, width ranges, and depth ranges (Supplementary Information, Supplementary Figs. S4–S7).

We located four large gorge and valley systems in the bathymetric data in addition to the Lambeck and Malita Valleys. We measured the depths, widths, and lengths of all features, and took elevation profiles at three intervals along their lengths to visualise morphology (Supplementary Information, Supplementary Figs. S8–S13). We found regional, undrowned comparative examples of the Northwest Shelf gorge systems by projecting the *1 s SRTM Level 2 Derived Digital Elevation Model v1.0* (Gallant et al., 2009) in ArcGIS Pro. We visually examined the topography of the escarpment regions of the Kimberley and Western Arnhem Land for similar gorge features to those found in the bathymetry of the Northwest Shelf. Once we identified examples, we compared their length, width, depth, and elevation profiles (Supplementary Figs. S8–S13, Supplementary Fig. S14). We identified the Kimberly Depression from elevation profiles across the Bonaparte Basin, which showed a distinct intra-shelf depression to the southwest of the Malita intra-shelf basin. We identified the depression sill at the -80 m contour line, and measured maximum depth, width, and length, from which we calculated surface area.

2.3. Carrying capacity

We estimated the theoretical (potential) carrying capacity of the region based on net primary production derived from climate hindcasts at a resolution of $0.5^\circ \times 0.5^\circ$ for Northwest Sahul (9° – 133° S latitude, and 122° – 133° E longitude). We derived net primary production (kg C

$\text{m}^{-2} \text{year}^{-1}$) from the LOVECLIM Earth system model (Goosse et al., 2010) of intermediate complexity (Claussen et al., 2002) (i.e., its spatial resolution is coarser than that of state-of-the-art general circulation models, and its representation of physical processes is simpler). LOVECLIM includes representations of the atmosphere, ocean and sea ice, the terrestrial biosphere and oceanic carbon cycle, and produces climates over the past 800 ka in 1000-year snapshots that we downscaled (using a bilinear interpolation) (Lorenz et al., 2016; Wilby and Wigley, 1997) to a spatial resolution of $0.5^\circ \times 0.5^\circ$. Of course, the land area of Sahul changes with fluctuating sea levels, so we estimated exposed land in 1000-year time slices based on a digital elevation model and estimated sea level change over the period of interest for Marine Isotope Stages 4 (71 ka–59 ka) and 3 (58 ka–30 ka).

To translate the hindcasted net primary production (Timmermann and Friedrich, 2016) into a carrying capacity expressed in units of humans the landscape could support (Bradshaw et al., 2019), we used the predicted relationship between net primary production and human density for hunter-gatherer societies (Tallavaara et al., 2018). Here, we rescaled the net primary production values over all grid cells to concur with the minimum (0.018 km^{-2}) and maximum (1.152 km^{-2}) human densities over all of Sahul from 60 ka to the present, multiplied by cell area (3080.25 km^2) to give a per-cell K . This approach assumes a linear relationship between K and net primary production; however, a non-linear relationship where maximum K occurs at mid-range net primary production might be more realistic because ancient humans possibly struck a compromise between high productivity and ease of passage and/or visibility to hunt prey by tending toward ecotones of mid-range productivity (Finlayson et al., 2011). Therefore, we applied a 180° -rotated parabola model of the form:

$$K = -3(\text{NPP} - \text{NPP}_{\text{med}})^2 + K_{\text{max}}$$

where NPP = net primary production, and $K_{\text{max}} = 0.5K_{\text{max}}$ for the linear relationship, as well as a rotated quadratic yield-density model of the form:

$$K = \frac{\text{NPP}}{(200 + 0.6\text{NPP} + 0.2\text{NPP}^2)}$$

between K and net primary production (Fig. 2). For each relationship, we scaled the ΣK_{max} across all cells in Sahul and temporal layers to equal ΣK_{max} of the linear relationship (because of a higher frequency of cells with mid-range compared to high net primary production).

2.4. Artefact discard rates

We calculated and plotted artefact discard rates using primary data or graphical depictions of artefact counts and associated published ages. We provide artefact counts for Widgingarri 1 by technological phase, obtaining counts from Table 4 in Norman et al. (2022) and sourcing optical ages from Table 2. We obtained artefact concentrations by litre/excavation unit for Carpenter's Gap 1 from Fig. 7B, and representative calibrated radiocarbon age ranges for Square A2 from Table 3 in Maloney et al. (2018). We obtained artefact counts by depth and spit, and radiocarbon and luminescence ages for Goorurarmum-1 and Karlinga-3, from Figs. 3 and 4a, and from Table 1 of Ward et al. (2006). Jones and Johnson (1985) and Bird et al. (2002) provided artefact counts per kg sediment excavated for Nauwalabila by depth and ages. This enabled us to construct an age-depth curve to 20 ka (cf. Fig. 3 in Bird et al. (2002)) and assign a probable age to each spit. We then calculated discard rates per thousand years. Artefact counts for Madjedbebe by depth include data from Clarkson et al. (2017) Supplementary Table 13 and show optical ages (SW3B, SW2B, and SW4B) from Supplementary Table 5.

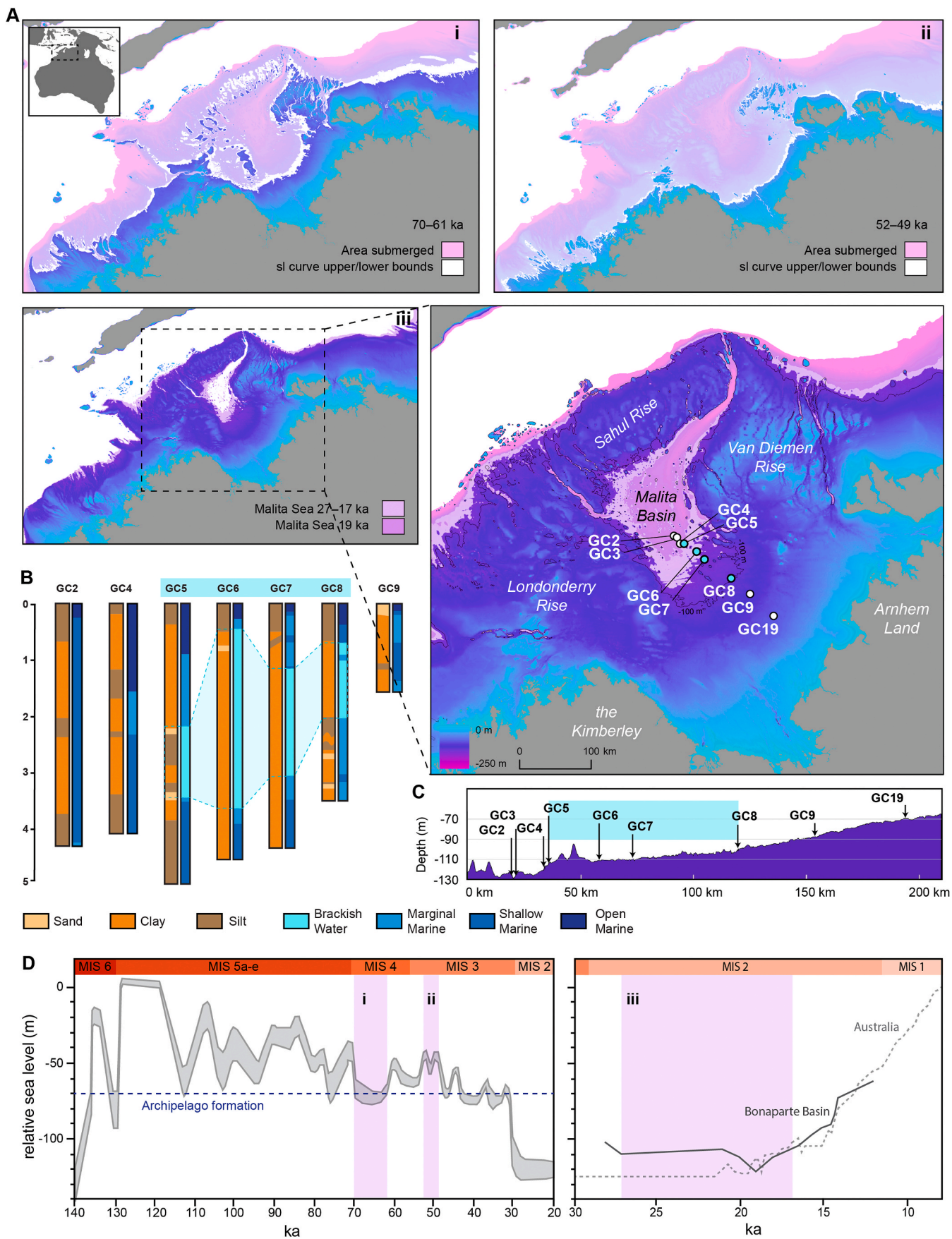
3. Results

3.1. Drowned landscapes of the shelf

The complex, low-lying Northwest Shelf experienced profound changes during the Late Pleistocene (Fig. 3). For the duration of Marine Isotope Stage 5 (130 ka–71 ka), higher sea levels meant much of the shelf was submerged, with a coastal morphology similar to that of today. The transition to Marine Isotope Stage 4 (71 ka–57 ka) produced a rapid drop in global sea levels of $\sim 40 \text{ m}$ (Lambeck and Chappell, 2001) (Fig. 3D), causing the carbonate platforms and terraces of the Londonderry, Sahul, and Van Diemen Rises to emerge (Fig. 3A and 3D). At that time, the Bonaparte Basin rapidly transformed from a vast embayment to a sweeping island archipelago (hereafter referred to as the Sahul Archipelago) (Fig. 3Ai). This event was the first time sea levels fell sufficiently to allow archipelago formation on the Northwest Shelf since Marine Isotope Stage 6 (191 ka–130 ka), some 60,000–70,000 years previously. The archipelago persisted for approximately 9000 years (70 ka–61 ka; Fig. 3Di) before submerging again in the second half of Marine Isotope Stage 4 with rising sea levels. Our use of the New Guinea Huon Terrace sea level curve (Lambeck and Chappell, 2001) is supported by analysis of seismic survey data from the Bonaparte Basin that indicate local sea levels were $\sim 80 \text{ m}$ in Marine Isotope Stage 4 (Fogg et al., 2022; Kuijjer et al., 2022), matching the lower bound of the sea level curve. Where possible, we compared sea-level curve projections on the bathymetric data of the Northwest Shelf to environmental proxy data (Methods, Supplementary Figs. S2–S3). Towards the end of Marine Isotope Stage 4, and with the onset of Marine Isotope Stage 3 (57 ka–29 ka), several rapid reversals in eustatic sea level produced highstand events at $\sim 60 \text{ ka}$ and 52–49 ka. Almost full inundation of the Londonderry and Sahul Rises occurred, with only the archipelago of the Van Diemen Rise persisting in the north-eastern Bonaparte Basin (Fig. 3Aii). Gravity cores GC2, GC4, GC5, GC8, and GC9, which contain the earliest dated material, extend from the centre of the Malita Basin in a south-eastern transect and show shallow and marginal marine environments from ~ 40 to 27 ka (Supplementary Fig. S2, Supplementary Table S2). Those environments date to a time in late Marine Isotope Stage 3 when the coastal morphology of the Bonaparte Basin closely resembled that in the Marine Isotope Stage 4 lowstand, with a second extended period of archipelago formation.

The termination of Marine Isotope Stage 3 and the onset of Stage 2 (29 ka–14 ka) produced a regional fall to $\sim 120 \text{ m}$ relative sea level in the Bonaparte Basin at the peak of the Last Glacial Maximum (Ishiwa et al., 2019). The Last Glacial Maximum is a period of global ice sheet maxima and thermal minima spanning 26.5 ka–19 ka (Clark et al., 2009), with the peak of the small glaciation occurring in Australia between 20 ka and 17 ka (Barrows et al., 2002). The descent into full glacial conditions produced a rapid transition from an archipelago environment to a broad, fully exposed terrestrial shelf (Fig. 3Aiii). At that time, the Malita Sea formed in the Malita intra-shelf basin, resulting in a landlocked marine environment, with a marine connection only through the Malita Valley.

We found several major differences projecting the regional sea level curve for the Bonaparte Basin (Ishiwa et al., 2019) onto high-resolution bathymetric data (Beaman, 2018), compared to earlier studies for the glacial peak of Marine Isotope Stage 2 based on non-regional sea-level curves on lower-resolution bathymetry (Williams et al., 2018; Yokoyama et al., 2001b). Analysis reveals two phases for the Malita Sea during the Marine Isotope Stage 2 lowstand. First, a larger waterbody (surface area $\sim 18,500 \text{ km}^2$) existed for $\sim 10,000$ years from $\sim 27 \text{ ka}$ – 17 ka . Second, a smaller sea with a reduced surface area ($\sim 12,000 \text{ km}^2$) existed for a brief interval at 19 ka at the peak of the Last Glacial Maximum when sea levels were at their lowest. A transition from a shallow marine to marginal marine environment occurred at the edge of the deeper Malita Basin epicentre in cores GC4 and GC5 at $\sim 29 \text{ ka}$ – 27 ka , corresponding to falling sea levels with the onset of Marine Isotope Stage 2 (Supplementary Fig. S2). Core GC4 shows marginal marine



(caption on next page)

Fig. 3. A Bathymetric data showing the Northwest Sahul continental shelf with eustatic and regional sea level curves projected. **Ai** Coastline morphology during the Marine Isotope Stage 4 sea level lowstand (~70 ka–61 ka), and **Aii** during the Marine Isotope Stage 3 sea level highstand (~52 ka–49 ka). **Aiii** Coastline morphology during the Marine Isotope Stage 2 sea level lowstand (~27 ka–17 ka), with place names shown. **B** Sediment cores from the Bonaparte Basin showing the sequence of environmental facies (adapted from Yokoyama et al., 2001a; Yokoyama et al., 2001b). Full details of the specific nature of the lithofacies identified in the cores can be found in the relevant publications. **C** Core locations are shown along a surface transect of the Malita Basin, and in the expanded inset of **Aiii**. **D** Huon Terrace eustatic sea level curve (left panel) adapted from Lambeck and Chappell (2001). Bonaparte Basin regional sea-level curve (right panel, solid grey line) and Australian regional sea-level curve (dashed grey line) adapted from Ishiwa et al. (2019) and Williams et al. (2018). The Australian sea-level curve represents a line of best fit from the combined dataset of Lewis et al. (2013). Purple highlighted regions i–iii correspond to the marine inundation maps in Ai–iii. Bathymetric data: high-resolution depth model for Northern Australia –30 m (Beaman, 2018).

environments continued in the deepest part of the Malita Depression from ~27 ka to 19 ka. This was adjacent to a shallow, brackish estuarine/lagoonal environment detected in cores GC5 to GC8 (Yokoyama et al., 2001a) and dates to the brief period at the height of the Last Glacial Maximum when the Malita Sea shrank to its smallest extent, matching our projection (Supplementary Fig. S2). An elevation profile along the marine core transect shows brackish conditions initiated at an area of higher elevation at the edge of the Malita Basin's epicentre, with the estuarine/lagoonal environment from this point to the –100 m contour. This environment was likely shallow, with the GC5 core (the deepest location to show brackish facies) indicating water depths of <5 m (De Deckker and Yokoyama, 2009) (Fig. 3Aiii, and 3C, Supplementary Information). Results indicate that during most of the 10,000-year window (~27 ka–17 ka), the Malita Sea was a similar size to, but with a more restricted marine connection than, the modern-day Sea of Marmara in Turkey. Marginal marine conditions re-initiated at ~19 ka–17 ka across cores GC5–7, with GC19 registering an intertidal environment by 13 ka (Supplementary Figs. S2–S3, Table S2), also matching our projections.

Sediment cores show continental rivers and streams drained into the Malita Sea, with rivers remaining active throughout Marine Isotope Stage 2 (De Deckker and Yokoyama, 2009; Ishiwa et al., 2016b, 2019; van Andel et al., 1967; Yokoyama et al., 2000, 2001a). We reveal multiple palaeochannels clearly visible in the high-resolution bathymetric data across the broad, sloping plain that comprises much of the south-western to south-eastern half of the Bonaparte Basin (Fig. 4A and 4C, Supplementary Figs. S4–S7). These palaeochannels range in size from large (e.g., the 100-km long, 2-km wide palaeochannel to the north of the Victoria River mouth; Fig. S5), to small (e.g., the ~30-km long, ~100-m wide network of channels visible in the southeast of the Bonaparte Basin; Fig. 4Ci). The channels drained towards the Malita intra-shelf basin and into the extensive gorge and valley systems of the Van Diemen Rise (Fig. 4). Those channels likely incised during the Marine Isotope Stage 2 sea level lowstand when an erosional surface formed, capping Marine Isotope Stage 3 sea level highstand sediment sequences (Clarke and Ringis, 2000; Collins et al., 2011; James et al., 2004). Extensive palaeochannel development in the southwest of the Bonaparte has been dated to the Last Glacial Maximum (Clarke and Ringis, 2000; Clarke et al., 2001).

The complex topography of the northwest to northeast Bonaparte Basin is dominated by the deeply incised flat-topped plateaus of the Londonderry, Sahul, and Van Diemen Rises. These contain many gorge and valley systems, which in some cases connect to palaeochannels draining the continental shelf (Fig. 4A, 4Cii). During the Marine Isotope Stage 4 sea level lowstand, a marine connection was established with the gorges and valleys of the Londonderry and Van Diemen Rises, likely creating topographically and ecologically complex regions potentially containing vast estuarine environments reaching over 100 km inland (Fig. 3Ai). Regional modern analogues for the submerged gorges of the Northwest Shelf are Deaf Adder Gorge and East Alligator River Gorge in the Arnhem Land Plateau in western Arnhem Land (Fig. 4E, Supplementary Fig. S14). While both gorges are several tens of metres deeper and on average shorter in length than many on the drowned shelf, their elevation profile transects are similar to the gorge features on the Northwest Shelf (Fig. 4B and 4E, Supplementary Figs. S8–S13).

Five deep valley and gorge systems found across the Northwest Shelf had the greatest potential to act as permanent rivers and reservoirs for freshwater during times of lower sea level. They range in length from 30 km to >120 km, with steep-sided walls extending vertically 100–175 m from their base (Supplementary Figs. S8–S13). All five gorge and valley systems contain deep areas where fresh water could have pooled, as seen in many of the modern gorges in Arnhem Land today. A large palaeochannel is clearly visible in the bathymetry draining into a gorge system in the Van Diemen Rise (Fig. 4Cii; Supplementary Fig. S7). With freshwater runoff and fluvial input, these catchments had the potential to form freshwater reservoirs like those in Arnhem Land and the Kimberley today. If this occurred, the largest gorges of the Van Diemen Rise would have created a series of freshwater refugia across the landscape located ~100 km from one another (Fig. 4A). The Sahul Rise contains fewer and smaller features of this kind and functioned as an isolated catchment area due to its position to the north of the Malita Basin, with the Lambeck Valley creating a >100 km-long marine barrier on its western margin during Marine Isotope Stage 2. While the Londonderry Rise contained only one substantial valley system (Fig. 4A, Supplementary Fig. S13), an isolated sub-basin/depression to the southwest of the Malita intra-shelf basin (Fig. 5A) might have increased the regional freshwater availability.

Located ~30 km north of the modern-day Kimberley coastline is a ~12,500 km² depression (Fig. 5A and 5D) with lowest elevation at the south-eastern end where the topography dips to –100 m. First identified as a potential catchment basin by Yokoyama et al. (2001b), this feature remains unnamed, and so we call it the *Kimberley Depression* to reflect its hydrological relationship to that region. We find that when sea levels became higher than –80 m, the depression would have had a marine connection, with the entire region drowned through Marine Isotope Stages 5–3, with the sub-basin encircled by islands (Fig. 5E). During the Marine Isotope Stages 6 and 2 lowstands, sea level in the Bonaparte Basin dropped below the –80-m contour, with the depression becoming isolated from the marine environment of the Malita Basin for up to 16,000 years (~30 ka to ~14 ka; Fig. 5E). We identified a large palaeochannel adjacent to Cape Bougainville on the northern Kimberley coastline, which might be the palaeo-Lawley/Mitchell River channel. The palaeochannel had a northeast drainage pattern towards the Kimberley Depression (Fig. 5B, Supplementary Fig. S4). The King Edward, Drysdale, and King George River mouths also discharge into the Bonaparte Gulf 80–170 km farther east along the modern coastline, bringing them to within 20–70 km of the Kimberley Depression, and at 80 m elevation to it. Because the topography of the basin means even river channels as far west as the palaeo-Lawley/Mitchell River channel drained towards the Kimberley Depression, it is plausible that the discharge from all four major rivers flowed into the depression and fed a freshwater lake (Fig. 5A).

The potential extent of Lake Kimberley is shown at the –85 m contour (white contour), and could have covered ~2000 km². A lake of this size would have been half the size of Kati Thandi (Lake Eyre), ten times larger than Lake Mungo, and covered an area approximately the size of the entire Willandra Lakes system (Fig. 5C). If the putative lake exceeded the –80 m contour (black contour), it would have overspilled along two channels to the north and southeast (indicated by white arrows) and drained towards the Malita Sea. The existence of such a lake for

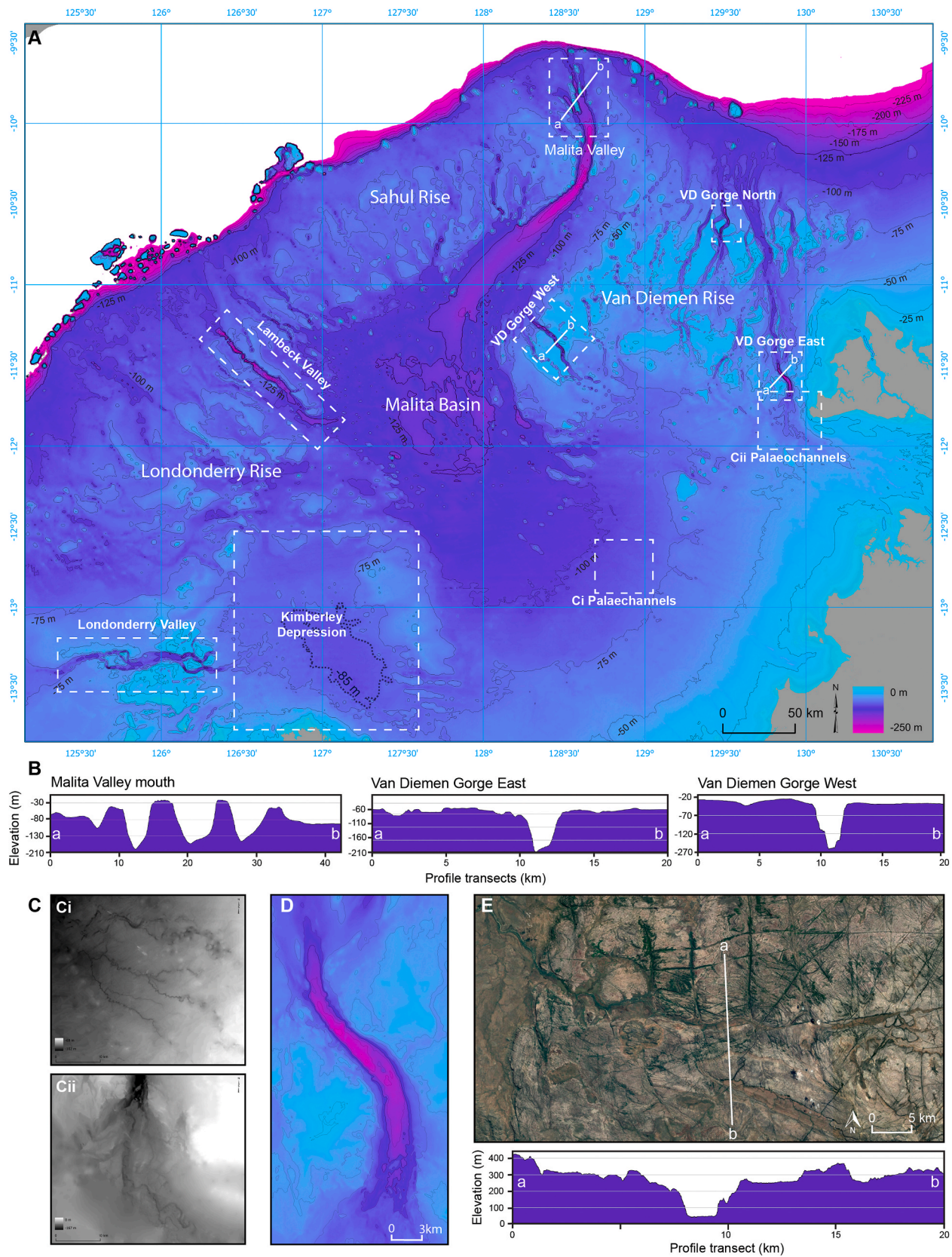


Fig. 4. A Continental shelf of Northwest Sahul with landscape features discussed in text demarcated by dashed white boxes. B Elevation profile transects of the Malita Valley mouth, and Van Diemen Gorge East and Van Diemen Gorge West. C Palaeochannels visible in bathymetric data. D Bathymetric data showing Van Diemen Gorge East. E Satellite imagery and elevation profile transect of Deaf Adder Gorge in western Arnhem Land. Bathymetric data: high-resolution depth model for Northern Australia –30 m (Beaman, 2018). Satellite imagery: Landsat image courtesy of the U.S. Geological Survey.

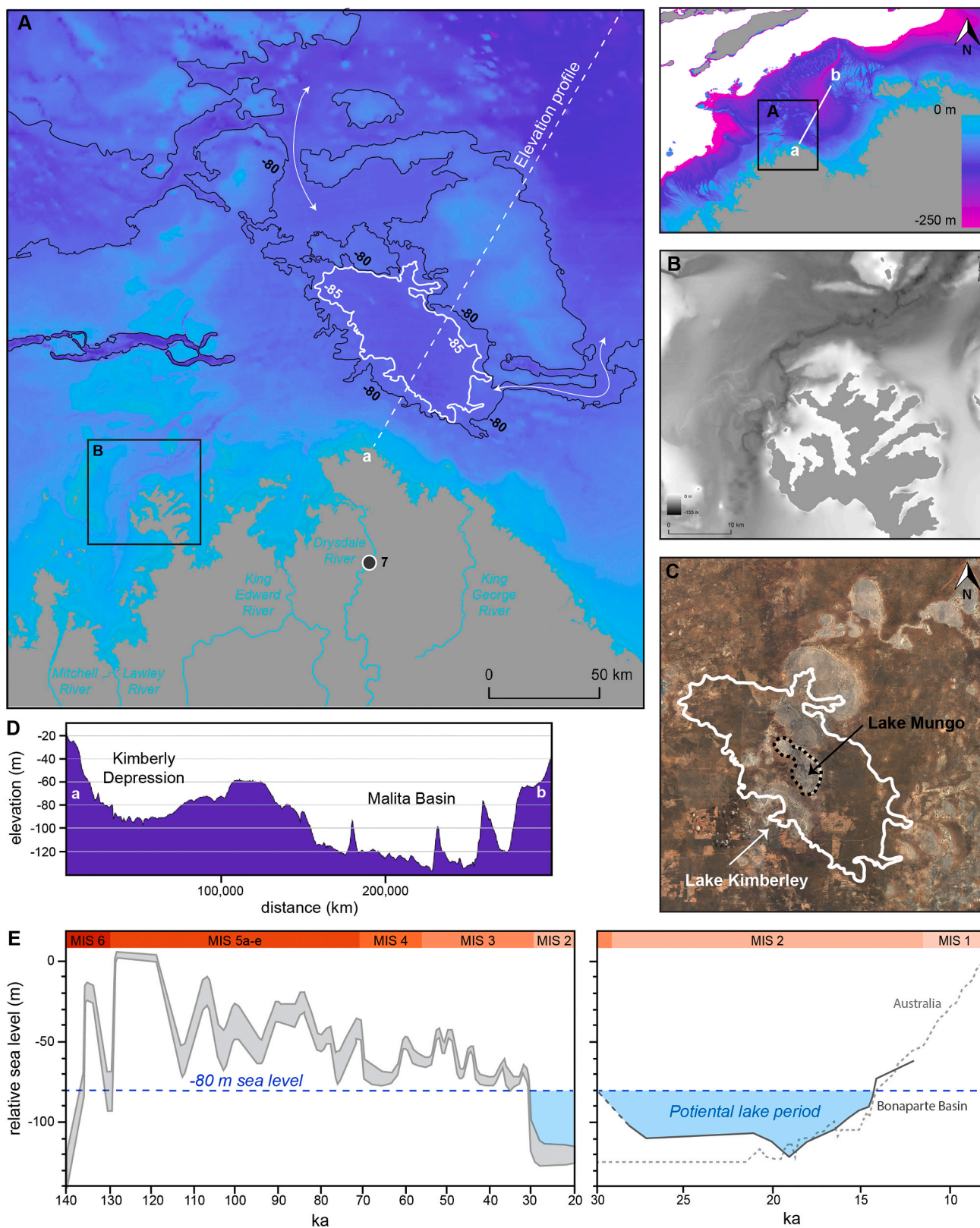


Fig. 5. Kimberley Depression and Lake Kimberley. **A** Bathymetric data showing the Kimberley Depression with potential maximum lake extent shown by the -85 m contour (white). Overflow of the lake or a marine incursion at times of rising sea level would occur once the -80 m contour (black) was breached. The major rivers draining the Kimberley are shown (the Mitchell, Lawley, King Edward, Drysdale, and King George Rivers). **B** Palaeochannel draining northwest toward the Kimberley Depression visible in the bathymetric data close to Cape Bougainville. **C** Satellite imagery of the Willandra Lakes with the putative Lake Kimberley (white line) overlain on Lake Mungo (black dashed line). **D** Elevation profile of the Kimberley Depression and the Malita Basin. **E** Marine Isotope Stages 6–1 sea levels with the window of potential lake formation shown in blue (left panel shows the eustatic sea level curve (Lambeck and Chappell, 2001), right panel the regional sea level curve (Ishiwata et al., 2019)). Bathymetric data: High-resolution depth model for Northern Australia - 30 m (Beaman, 2018). Satellite imagery: Landsat image courtesy of the U.S. Geological Survey.

approximately 16,000 years in Marine Isotope Stage 2 could have sustained a large freshwater ecosystem. Such an environment would have important implications for past human habitation of the region, potentially focusing human subsistence activities around its margins.

3.2. Human carrying capacity

Potential carrying capacity (K) as simulated from the hindcasted Earth system model expressed in units of people the Northwest Shelf was potentially capable of supporting per 1000-year interval over Marine Isotope Stage 4 (71 ka–59 ka), 3 (58 ka–30 ka) and 2 (29 ka–14 ka) suggests K fluctuated between 100,000 and almost 600,000 depending on the assumption of the underlying K -net primary production model and the Marine Isotope Stage (Fig. 6). The rotated parabola model estimates higher K than either the linear or rotated quadratic yield-density models, because of the high density of mid-range net primary-production cells within this region relative to the rest of Sahul (Fig. 2). The main feature is the reconstructed K time series — irrespective of the underlying model — was the decline in K during the descent into the Marine Isotope Stage 4 glacial (Fig. 6). With the onset of Marine Isotope Stage 3, the shelf was potentially capable of supporting between approximately one-quarter to half a million people between ~50 and 40 ka, declining towards the end of Marine Isotope Stage 3. These trends are evident despite taking into account the fluctuating shelf size in the model (albeit at a resolution of $0.5 \times 0.5^\circ$ latitude), with K increasing substantially even as rising sea levels drowned the Bonaparte Basin in Marine Isotope Stage 3. The second half of Marine Isotope Stage 3 again saw a substantial reduction in K , with a brief peak at the height of the Last Glacial Maximum in Marine Isotope Stage 2, potentially a result of the greatly increased shelf area. The model presented here functions as a useful heuristic for relative landscape potential carrying capacity rather than representing real-world population numbers.

3.3. Population retreat

Modelling carrying capacity of the Northwest Shelf indicates the region was capable of sustaining a large human population, with implications for the impact of post-glacial sea level rise. Two periods of rapid sea level rise follow the termination of the Last Glacial Maximum. The first occurred between 14.5 ka and 14.1 ka during Meltwater Pulse 1A (Ishiwata et al., 2019; Lambeck et al., 2014; Lin et al., 2021), with sea level rise increasing from 1 m per hundred years to 4–5 m per hundred years (Fig. 7A). This sudden rapid increase in the pace of sea level rise

drowned >100,000 km² of land in the space of 400 years, having a profound impact within the scale of a human lifespan (Fig. 7B). The second more protracted period of rapid sea level rise spanned ~12 ka–9 ka, with the onset of the Holocene experiencing repeated pulses, drowning another >100,000 km² of land over a 3000-year interval (Fig. 7A and B).

Those two periods of accelerated sea level rise and associated drowning of vast areas of the Northwest Shelf register as a pulse in occupational intensity in archaeological sites across the Kimberley and Arnhem Land. Occupational intensity can be measured in various ways, including changes in the discard of stone artefacts at a site through time. This is particularly useful where alternative measures are unavailable, such as large numbers of ages, rich faunal assemblages or obvious transformations in habitation space to accommodate larger groups. If numbers of objects at a site are a proxy for population size, as argued previously (Bradshaw et al., 2021; Williams et al., 2013, 2018; Williams, 2013), then at many northern Australian rockshelters where organic preservation is poor, stone artefacts are the most appropriate form of cultural material with which to quantify changes in the number of people and/or frequency of habitation through time (Attenbrow, 2007; Clarkson, 2007; Hiscock, 1981). Analysis of artefact discard rates from six rockshelters in the Kimberley (Maloney et al., 2018; Norman et al., 2022; Ward et al., 2005, 2006) ($n = 4$) and Arnhem Land (Clarkson et al., 2017; Jones and Johnson, 1985; Roberts et al., 1994) ($n = 2$) for which ages and artefact counts are available (see Methods), indicates increasing artefact discard leading up to two peaks in discard at 14 ka and 12 ka–9 ka (Fig. 7C). Pulse 1 registered as a peak in occupational intensity at 13.9 ± 1 ka at Widgingarri 1 (Norman et al., 2022) and at 14.3 ± 0.6 ka at Goorurarmum 1 (Ward et al., 2005, 2006) in the Kimberley. Pulse 2 (12–9 ka) registered at sites in both the Kimberley and Arnhem Land (Fig. 7B and 7C). We interpret increases in discard as reflecting an influx of people ahead of a rapidly encroaching coastline. In the two cases (Madjedbebe: Clarkson et al. (2017) and Widgingarri 1: Norman et al. (2022) where detailed artefact descriptions exist, there is evidence for a shift toward bipolar technology. At Nauwalabila I (Jones and Johnson, 1985; Roberts et al., 1994), there was also a shift from chert to quartz that is possibly associated with greater use of bipolar technology (although bipolar artefacts were not counted in Jones and Johnson (1985)). The shift to bipolar technology likely indicates higher mobility and greater unpredictability of resource acquisition as sea levels rose rapidly and people were displaced or migrated into new environments (Hiscock, 1994).

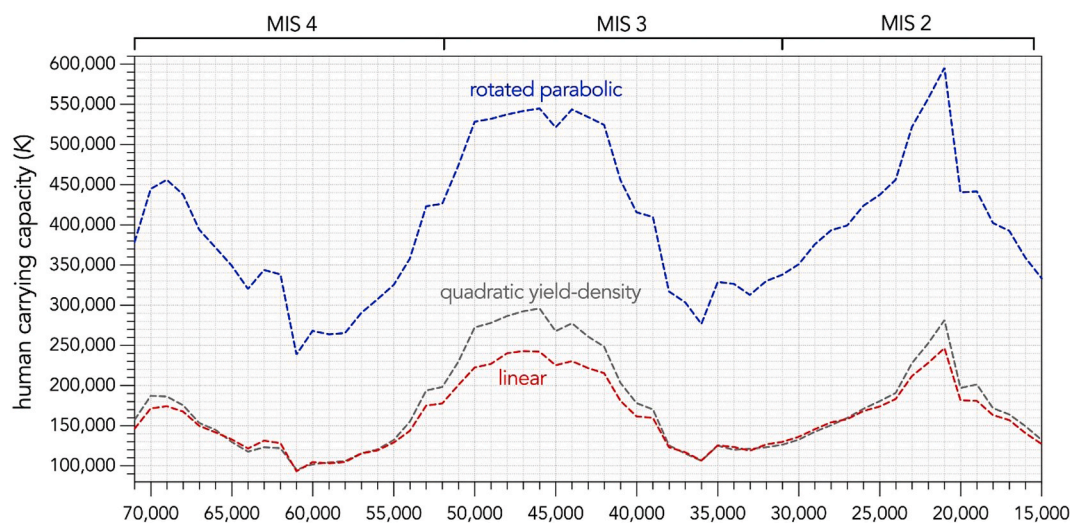


Fig. 6. Putative carrying capacities (K) reconstructed for the Northwest Shelf represented by carrying capacity in units of people is shown for the period spanning Marine Isotope Stages 4–2 (71 ka–14 ka).

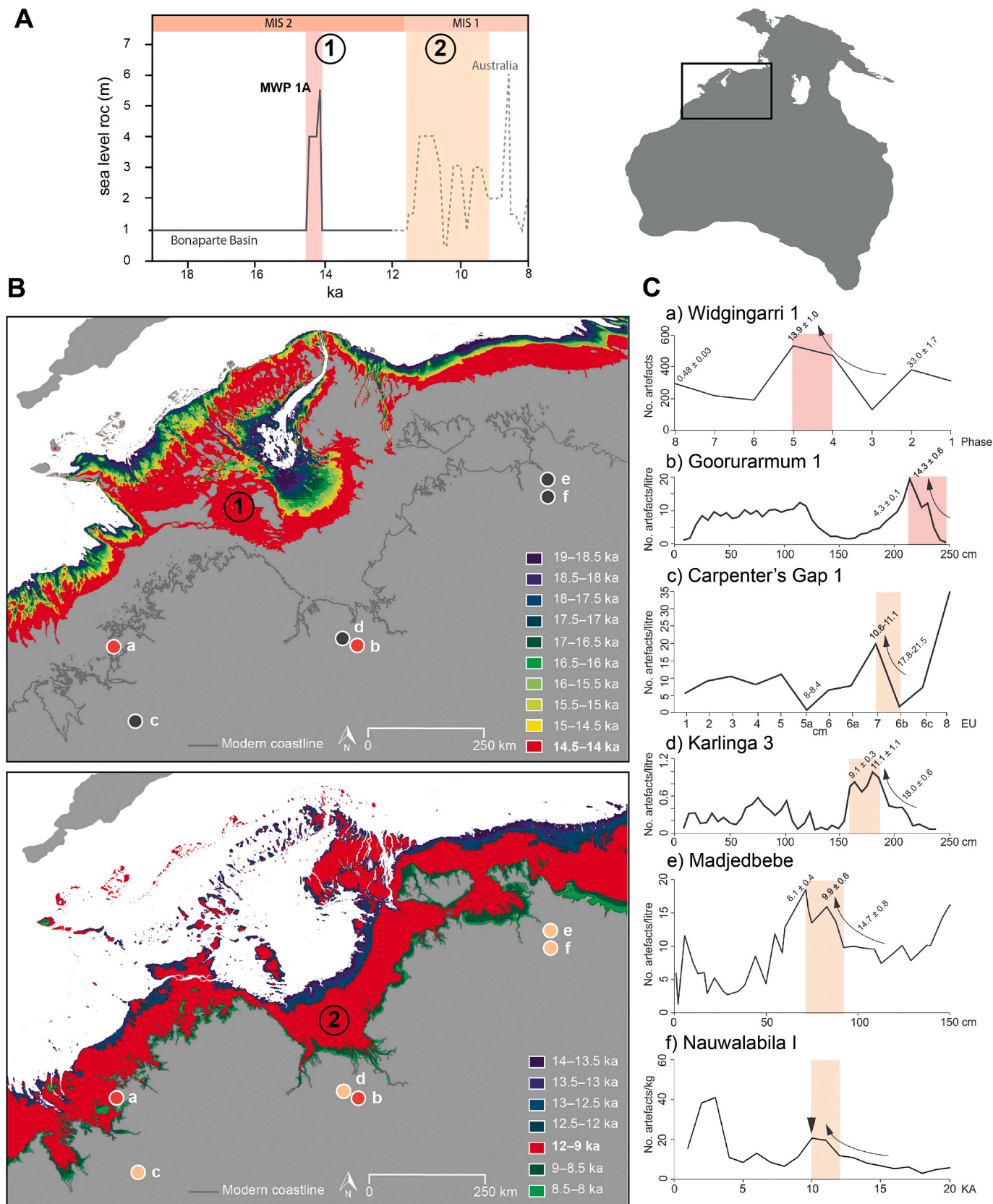


Fig. 7. A Rate of change of sea-level rise (m of sea level rise per 200 year increment) adapted from Ishiwa et al. (2019) and Williams et al. (2018). Accelerated sea level rise occurs during Meltwater Pulse 1A, and during a series of rapid pulses with the onset of the Holocene. B Sea level rise for the Northwest Shelf projected onto high-resolution bathymetric data in 500-year increments, with periods of rapid sea level rise and land submergence in red. Archaeological sites registering a corresponding pulse in occupation are in red (Pulse 1) and brown (Pulse 2), with site letters a–f relating to panel C. C Artefact discard rates at sites in the Kimberley and Arnhem Land with pulses in discard rates that correspond to rapid sea-level rise highlighted (Pulse 1: red; Pulse 2: brown). Bathymetric data: High-resolution depth model for Northern Australia - 30 m (Beaman, 2018).

4. Discussion

The mounting archaeological evidence from around the continental margin of Sahul suggests that the First Australians used the Late Pleistocene and early Holocene landscapes and environments of the now-submerged Sahul continental shelves (Benjamin et al., 2020; Bowdler, 1975; Ditchfield et al., 2022; Hope et al., 1977; Neal and Stock, 1986; Veth, 2017). However, several arguments have focused on the potentially unproductive nature of these environments (Beaton, 1985, 1995; Bowdler, 2010; Callaghan, 1980). The Northwest Shelf is shown to be a geographically complex region, transitioning from a vast archipelago in Marine Isotope Stage 4 to an expansive embayment in Marine Isotope Stage 3, backed by the broad sloping plains of the continental shelf. Drier conditions than today prevailed at the transition of Marine Isotope Stage 3 to Stage 2 (Kemp et al., 2019; Marx et al., 2021), with precipitation gradually increasing throughout the latter, and an active (although variable) monsoon (Denniston et al., 2013; Florin et al., 2021; Maloney et al., 2018; Rowe et al., 2021). During Marine Isotope Stage 2, the fully exposed shelf contained a vast inland sea potentially adjacent to a large lake, both encircled by escarpments cut by deep gorges, and broad sloping plains incised by river systems. Palaeoenvironmental records show river systems draining the continent continued to discharge into the Northwest Shelf and Malita Basin throughout this period (De Deckker and Yokoyama, 2009; Ishiwa et al., 2016a, 2019; Yokoyama et al., 2000, 2001a). We contend that the exposed Northwest Shelf contained diverse and productive environments in both Marine Isotope Stage 4 and Stage 2 that were potentially in place for ~9000 and ~10,000 years, respectively. Our evidence for rich and varied niches on the continental shelf has broad implications for the success of the initial peopling of Sahul as well as the speed and direction of settlement, and highlights a need to reconstruct the palaeoecology of the shelf in sophisticated ways.

While our understanding of the timing of the initial human dispersal through Wallacea to Sahul is still evolving (Norman et al., 2021), the Marine Isotope Stage 4 sea level lowstand (~70 ka–61 ka) represents a best-case maritime-crossing window from the Wallacean islands of Timor and Roti to the Northwest Shelf (Bird et al., 2018; Kuijjer et al., 2022; Norman et al., 2018). With the Sahul Archipelago stable for an approximate 9000-year window, the region contained a contiguous maritime island environment for people to disperse into from the Wallacean archipelago. The ability to cross from one island environment to another would have allowed the first maritime explorers to transition their Wallacean adapted maritime economies to Sahul, with the first interaction with the new continent taking place in an environment type with which they were already familiar. Such a scenario postulates a phased transition from the maritime adapted economies necessary for a successful human dispersal through Wallacea, to those required for expansion across the vast terrestrial Sahul continental landmass with its unique flora and fauna.

A human response to the dynamic environments of the Northwest Shelf is detectable in the archaeological records of the adjoining Kimberley and Western Arnhem Land regions, with a pulse in first occupation appearing at multiple sites (Balme et al., 2019; Maloney et al., 2018; Norman et al., 2022; Veth et al., 2019; Wood et al., 2016) across the Kimberley following the Marine Isotope Stage 3 sea-level highstand (~52–49 ka). We postulate the onset of occupation across the Kimberley following this event potentially represents populations retreating inland in response to extensive marine flooding of the shelf at this time. There is a subsequent decrease in new site establishment rates in the Kimberley in Marine Isotope Stage 2 (Norman et al., 2022), a time when the putative Lake Kimberley might have created a highly productive freshwater environment to the north of the region. Population retreat to well-watered refugia areas during Marine Isotope Stage 2 occurred at multiple sites across northern Australia (Clarkson et al., 2017; Florin et al., 2021; Hiscock, 1984; Maloney et al., 2018). After this long period of shelf stability, the two periods of rapid sea-level rise (~14.5 ka–14.1

ka and 12 ka–9 ka) coincided with pronounced peaks in artefact discard rates and the emergence of distinctive new rock art styles in the Kimberley and Western Arnhem Land.

In Western Arnhem Land, a plethora of new art styles dominated by anthropomorphic imagery, overlying the early Large Naturalistic Fauna/Large Naturalistic Animals emerged during the Middle/Intermediate Period (Finch et al., 2020; Jones, 2017, Jones et al., 2017; Taçon et al., 2020; Walsh, 2000) (Fig. 1). In Arnhem Land, this included Dynamic Figures and later anthropomorphic stylistic variants such as Post Dynamic Figures, Simple Figures with Boomerangs, Maliwawa figures, Northern Running Figures, Yam Figures, and Simple Figures. An absolute minimum age of 9.4 ka for the Northern Running Figures art style provides a minimum age for the introduction of anthropomorphic dominated styles, with Dynamic Figures occurring earlier in the relative painting sequence, with the timing of the introduction of Dynamic Figures argued to coincide with Meltwater Pulse 1A. It is also in the Middle/Intermediate Period that scenes of activity appear. Rock art panels depicting scenes of between 50 and 70 figures, often in opposing groups have been argued to depict conflict/battle scenes (Tacon and Chippindale, 1994), or the depictions of ritual behaviours and the spiritual lives of ancient populations (Johnston, 2018; May et al., 2018). If these scenes of activity do depict conflict, the rock art then could be literal depictions arising from demographic concentration, resource access and availability as sea levels rose. Similar scenes of activity are identified in the terminal Pleistocene Gwion rock art of the Kimberley region (Walsh, 2000).

5. Conclusion

Our findings that the Northwest Shelf of Sahul likely contained a rich and varied sequence of mosaic environments through Marine Isotope Stages 4–2 have implications for the successful transition made by the first Australians from island Wallacea to Sahul. It is clear that the temptation to ignore the continental shelf margins of Late Pleistocene Sahul in debates of early peopling and expansion carries the risk of both oversimplifying and misunderstanding important elements of this period of history. Our analysis indicates the Northwest Shelf was a large habitable landscape that connected the now-separated ancient archaeological landscapes of the Kimberley and Arnhem Land. Reconstructing the palaeoecology of these landscapes in sophisticated ways remains an important goal for future research to understand the potential lifeways of the First Australians. The appearance of new and distinctive rock art styles in the Kimberley and Arnhem Land coincides with major shelf-drowning events and a noticeable increase in stone artefact discard across both regions. We interpret this as the retreat of human populations from the Northwest Shelf as sea levels rose. Now submerged continental margins clearly played an important role in early human expansions across the world. The rise in undersea archaeology in Australia will contribute to a growing worldwide picture of early human migration and the impact of climate change on Late Pleistocene human populations.

CRediT authorship contribution statement

Kasih Norman: Conceptualization, Methodology, Formal analysis, Investigation, Writing - original draft, Writing - review & editing, Visualization. **Corey J.A. Bradshaw:** Methodology, Formal analysis, Writing - review & editing, Visualization. **Frédéric Saltré:** Methodology, Formal analysis, Writing - review & editing. **Chris Clarkson:** Investigation, Writing - review & editing. **Tim J. Cohen:** Supervision, Writing - review & editing. **Peter Hiscock:** Supervision, Writing - review & editing. **Tristen Jones:** Writing - review & editing. **Fabian Boesl:** Formal analysis.

Declaration of competing interest

The authors declare that they have no known competing financial interests or personal relationships that could have appeared to influence the work reported in this paper.

Data availability

The processed data required to reproduce the above findings are available to download from <https://ecat.ga.gov.au/geonetwork/srv/eng/catalog.search#/metadata/121620> and <https://elevation.fsdf.org.au/>.

Acknowledgments

This study was funded by the Australian Research Council through a Centre of Excellence Grant (CE170100015) to T.C. and C.J.A.B., and an Australian Government Research Training Program Award to K.N. We thank our reviewers for their helpful comments on improving the paper.

Appendix A. Supplementary data

Supplementary data to this article can be found online at <https://doi.org/10.1016/j.quascirev.2023.108418>.

References

- Anderson, T.J., et al., 2011. Seabed Environments of the Eastern Joseph Bonaparte Gulf, Northern Australia. Geoscience Australia, Canberra.
- Attenbrow, V., 2007. What's Changing: Population Size or Land-Use Patterns? The archaeology of Upper Mangrove Creek, Sydney Basin. In: Terra Australis, 21. ANU E Press, Canberra.
- Balme, J., et al., 2019. Long-term occupation on the edge of the desert: Riwi Cave in the southern Kimberley, Western Australia. *Archaeol. Ocean.* 54, 35–52. <https://doi.org/10.1002/arco.5166>.
- Barrows, T.T., Stone, J.O., Fifield, L.K., Cresswell, R.G., 2002. The timing of the last glacial maximum in Australia. *Quat. Sci. Rev.* 21, 159–173. [https://doi.org/10.1016/S0277-3791\(01\)00109-3](https://doi.org/10.1016/S0277-3791(01)00109-3).
- Bayón, M.C., Politis, G.G., 2014. The inter-tidal zone site of La Olla: early–middle Holocene human adaptation on the Pampean Coast of Argentina. In: Evans, A., Flatman, J., Flemming, N. (Eds.), *Prehistoric Archaeology on the Continental Shelf*. Springer, New York, pp. 115–130. <https://doi.org/10.1007/978-1-4614-9635-9>.
- Beaman, R.J., 2018. In: High-resolution depth model for Northern Australia - 30 m. Geoscience Australia, Canberra. <https://doi.org/10.4225/25/5b35b3b8074a9>.
- Beaton, J.M., 1985. Evidence for a coastal occupation time-lag at Princess Charlotte Bay (North Queensland) and implications for coastal colonization and population growth theories for Aboriginal Australia. *Archaeol. Ocean.* 20, 1–20.
- Beaton, J.M., 1995. The Transition on the coastal fringe of Greater Australia. *Antiquity* 69, 798–806. <https://doi.org/10.1017/S0003598X0008234X>.
- Belde, J., Back, S., Bourget, J., Reuning, L., 2017. Oligocene and Miocene carbonate platform development in the Browse Basin, Australian Northwest Shelf. *J. Sediment. Res.* 87, 795–816. <https://doi.org/10.2110/jsr.2017.44>.
- Benjamin, J., et al., 2018. Underwater archaeology and submerged landscapes in Western Australia. *Antiquity* 92, 1–9. <https://doi.org/10.15184/aqy.2018.103>.
- Benjamin, J., et al., 2020. Aboriginal artefacts on the continental shelf reveal ancient drowned cultural landscapes in northwest Australia. *PLoS One* 15, e0233912. <https://doi.org/10.1371/journal.pone.0233912>.
- Benjamin, J., et al., 2023. Stone artefacts on the seabed at a submerged freshwater spring confirm a drowned cultural landscape in Murujuga, Western Australia. *Quat. Sci. Rev.* 313, 108190. <https://doi.org/10.1016/j.quascirev.2023.108190>.
- Bicket, A., Tizzard, L., 2015. A review of the submerged prehistory and palaeolandscapes of the British Isles. *Proc. Geologists' Assoc.* 126, 643–663. <https://doi.org/10.1016/j.pgeola.2015.08.009>.
- Bird, M., et al., 2002. Radiocarbon analysis of the early archaeological site of Nauwalabila I, Arnhem Land, Australia: implications for sample suitability and stratigraphic integrity. *Quat. Sci. Rev.* 21, 1061–1075. [https://doi.org/10.1016/S0277-3791\(01\)00058-0](https://doi.org/10.1016/S0277-3791(01)00058-0).
- Bird, M.I., et al., 2018. Palaeogeography and voyage modeling indicates early human colonization of Australia was likely from Timor-Roti. *Quat. Sci. Rev.* 191, 431–439. <https://doi.org/10.1016/j.quascirev.2018.04.027>.
- Bourget, J., Ainsworth, R., Backé, G., Keep, M., 2012. Tectonic evolution of the northern Bonaparte Basin: impact on continental shelf architecture and sediment distribution during the Pleistocene. *Aust. J. Earth Sci.* 59, 877–897. <https://doi.org/10.1080/08120099.2012.674555>.
- Bowdler, S., 1975. Further radiocarbon dates from Cave Bay Cave, hunter island, northwest Tasmania. *Aust. Archaeol.* 3, 24–26. <https://doi.org/10.1080/03122417.1975.12093278>.
- Bowdler, S., 2010. The empty coast: conditions for human occupation in southeast Australia during the late Pleistocene. In: Haberle, S.G., Stevenson, J., Prebble, M. (Eds.), *Altered Ecologies: Fire, Climate and Human Influence on Terrestrial Landscapes*. Terra Australis 32. ANU Press, Canberra, pp. 177–185. https://doi.org/10.26530/OAPEN_458799.
- Bradshaw, C.J.A., et al., 2019. Minimum founding populations for the first peopling of Sahul. *Nature Ecology & Evolution* 3, 1057–1063. <https://doi.org/10.1038/s41559-019-0902-6>.
- Bradshaw, C.J.A., et al., 2021. Stochastic models support rapid peopling of Late Pleistocene Sahul. *Nat. Commun.* 12, 2440. <https://doi.org/10.1038/s41467-021-21551-3>.
- Bradshaw, C.J.A., et al., 2023. Directionally supervised cellular automaton for the initial peopling of Sahul. *Quat. Sci. Rev.* 303, 107971. <https://doi.org/10.1016/j.quascirev.2023.107971>.
- Callaghan, M., 1980. Some previously unconsidered environmental factors of relevance to south coast prehistory. *Aust. Archaeol.* 11, 43–49. <https://doi.org/10.1080/03122417.1980.12092776>.
- Chaloupka, G., 1993. *Journey in Time: the 50,000 Year Story of the Australian Rock Art of Arnhem Land*. Reed Books Australia.
- Clarke, J., et al., 2001. Post-glacial biota from the inner part of southwest Joseph Bonaparte Gulf. *Aust. J. Earth Sci.* 48, 63–79. <https://doi.org/10.1046/j.1440-0952.2001.00845.x>.
- Clarke, J., Ringis, J., 2000. Late Quaternary stratigraphy and sedimentology of the inner part of southwest Joseph Bonaparte Gulf. *Aust. J. Earth Sci.* 47, 715–732. <https://doi.org/10.1046/j.1440-0952.2000.00804.x>.
- Clark, P.U., et al., 2009. The Last Glacial Maximum. *Science* 325, 710–714. <https://doi.org/10.1126/science.1172873>.
- Clarkson, C., 2007. Lithics in the Land of the Lightning Brothers: the Archaeology of Wardaman Country, Northern Territory. ANU Press, Canberra. https://doi.org/10.26530/OAPEN_459360.
- Clarkson, C., et al., 2017. Human occupation of northern Australia by 65,000 years ago. *Nature* 547, 306–310. <https://doi.org/10.1038/nature22968>.
- Clarkson, C., et al., 2022. Australia's First People: Oldest Sites and Early Culture. In: McNiven, Ian, J., Bruno, David (Eds.), *The Oxford Handbook of the Archaeology of Indigenous Australia and New Guinea*. Oxford University Press, pp. 241–272. <https://doi.org/10.1093/oxfordhb/9780190095611.013.9>.
- Claussen, M., et al., 2002. Earth system models of intermediate complexity: closing the gap in the spectrum of climate system models. *Clim. Dynam.* 18, 579–586. <https://doi.org/10.1007/s00382-001-0200-1>.
- Clendon, M., 2006. Reassessing Australia's linguistic prehistory. *Curr. Anthropol.* 47, 39–60. <https://doi.org/10.1086/497671>.
- Collins, L., Testa, V., Zhao, J., Qu, D., 2011. Holocene growth history and evolution of the Scott Reef carbonate platform and coral reef. *J. Roy. Soc. West Aust.* 94, 239–250.
- Courgeon, S., Bourget, J., Jorry, S.J., 2016. A Pliocene–Quaternary analogue for ancient epicritic carbonate settings: the Malita intrashelf basin (Bonaparte Basin, northwest Australia). *AAPG Bull.* 100, 565–595. <https://doi.org/10.1306/02011613196>.
- De Deckker, P., Yokoyama, Y., 2009. Micropalaeontological evidence for late Quaternary sea-level changes in Bonaparte Gulf, Australia. *Global Planet. Change* 66, 85–92. <https://doi.org/10.1016/j.gloplacha.2008.03.012>.
- Denniston, R.F., et al., 2013. North Atlantic forcing of millennial-scale Indo-Australian monsoon dynamics during the Last Glacial period. *Quat. Sci. Rev.* 72, 159–168. <https://doi.org/10.1016/j.quascirev.2013.04.012>.
- Ditchfield, K., et al., 2022. Framing Australian Pleistocene coastal occupation and archaeology. *Quat. Sci. Rev.* 293, 107706. <https://doi.org/10.1016/j.quascirev.2022.107706>.
- Dixon, R.M., 1997. *The Rise and Fall of Languages*. Cambridge University Press, Cambridge.
- Finch, D., et al., 2020. 12,000-Year-old Aboriginal rock art from the Kimberley region, Western Australia. *Sci. Adv.* 6, eaay3922. <https://doi.org/10.1126/sciadv.aay3922>.
- Finch, D., et al., 2021. Ages for Australia's oldest rock paintings. *Nat. Human Behav.* 5, 310–318. <https://doi.org/10.1038/s41562-020-01041-0>.
- Finlayson, C., et al., 2011. The *Homo* habitat niche: using the avian fossil record to depict ecological characteristics of Palaeolithic Eurasian hominins. *Quat. Sci. Rev.* 30, 1525–1532. <https://doi.org/10.1016/j.quascirev.2011.01.010>.
- Flemming, N.C., 1982. *Sirius Expedition-Cootamundra Shoals Survey 1982: Expedition Reports*.
- Flemming, N.C., 1983. *A Survey of the Late Quaternary Landscape of the Cootamundra Shoals, North Australia: a Preliminary Report*, pp. 149–180.
- Florin, S.A., et al., 2021. *Pandanus* nutshell generates a palaeoprecipitation record for human occupation at Madjedbebe, northern Australia. *Nature Ecology & Evolution* 5, 295–303. <https://doi.org/10.1038/s41559-020-01379-8>.
- Fogg, A., Dix, J., Farr, H., 2022. *Late Pleistocene Palaeo Environment Reconstruction from 3D Seismic Data, NW Australia*. The ACROSS Project-Australasian Research: Origins of Seafaring to Sahul. Earth and Space Science Open Archive.
- Gaffney, V., et al., 2017. *Doggerland and the lost frontiers project (2015–2020)*. In: Bailey, G.N., Harff, J., Sakellariou, D. (Eds.), *Under the Sea: Archaeology and Palaeolandscapes of the Continental Shelf*. Springer, Cham, pp. 305–319.
- Gaili, E., et al., 1993. Atlit-Yam: A Prehistoric Site on the Sea Floor off the Israeli Coast. *J. Field Archaeol.* 20, 133–157. <https://doi.org/10.1179/jfa.1993.20.2.133>.
- Gallant, J., Dowling, T., Read, A., 2009. 1 second SRTM Level 2 Derived Digital Elevation Model v1.0. Geoscience Australia, Canberra. <https://pid.geoscience.gov.au/dataset/ga/69816>.
- Golson, J., 2001. *New Guinea, Australia and the Sahul connection*. In: Anderson, Atholl, Lilley, Ian, O'Connor, Sue (Eds.), *Histories of old ages: essays in honor of Rhys Jones*.

- Pandanus Books, Research School of Pacific and Asian Studies. The Australian National University, pp. 185–210.
- Goosse, H., et al., 2010. Description of the Earth system model of intermediate complexity LOVECLIM version 1.2. *Geosci. Model Dev. (GMD)* 3, 603–633. <https://doi.org/10.5194/gmd-3-603-2010>.
- Groube, L., 1986. Waisted axes of Asia, Melanesia and Australia. In: Ward, G.K. (Ed.), *Archaeology at ANZAAS Canberra*. Canberra Archaeological Society, pp. 168–177.
- Heap, A., Przeslawski, R., Radke, L., Trafford, J., Battershill, C., 2010. Seabed Environments of the Eastern Joseph Bonaparte Gulf, Northern Australia: SOL4934 Post-Survey Report. Geoscience Australia, Canberra.
- Heaton, T.J., et al., 2020. Marine20—the marine radiocarbon age calibration curve (0–55,000 cal BP). *Radiocarbon* 62, 779–820. <https://doi.org/10.1017/rdc.2020.68>.
- Hiscock, P., 1981. Comments on the Use of Chipped Stone Artefacts as a Measure of 'Intensity of Site Usage'. *Aust. Archaeol.* 13, 30–34. <https://doi.org/10.1080/03122417.1981.12092820>.
- Hiscock, P., 1984. A preliminary report on the stone artefacts from Colless Creek Cave, northwest Queensland. *Queensland Archaeological Research* 1, 120–151.
- Hiscock, P., 1994. Technological responses to risk in Holocene Australia. *J. World Prehistory* 8, 267–292.
- Hope, J., Lampert, R., Edmondson, E., Smith, M., Van Tets, G., 1977. Late Pleistocene faunal remains from Seton Rock Shelter, Kangaroo Island, South Australia. *J. Biogeogr.* 4, 363–385. <https://doi.org/10.2307/3038194>.
- Ishiwa, T., et al., 2019. A sea-level plateau preceding the Marine Isotope Stage 2 minima revealed by Australian sediments. *Sci. Rep.* 9, 6449. <https://doi.org/10.1038/s41598-019-42573-4>.
- Ishiwa, T., Yokoyama, Y., Miyairi, Y., Ikehara, M., Obrochta, S., 2016a. Sedimentary environmental change induced from late Quaternary sea-level change in the Bonaparte Gulf, northwestern Australia. *Geoscience Letters* 3, 1–11.
- Ishiwa, T., et al., 2016b. Reappraisal of sea-level lowstand during the Last Glacial Maximum observed in the Bonaparte Gulf sediments, northwestern Australia. *Quat. Int.* 397, 373–379. <https://doi.org/10.1186/s40562-016-0065-0>.
- James, N.P., Bone, Y., Kyser, T.K., Dix, G.R., Collins, L.B., 2004. The importance of changing oceanography in controlling late Quaternary carbonate sedimentation on a high-energy, tropical, oceanic ramp: north-western Australia. *Sedimentology* 51, 1179–1205. <https://doi.org/10.1111/j.1365-3091.2004.00666.x>.
- Johnston, I.G., 2018. *The Dynamic Figure Art of Jabiluka: A Study of Ritual in Early Australian Rock Art*. Unpublished PhD Thesis. The Australian National University, Canberra Australia.
- Jones, T., 2017. *Disentangling the Styles, Sequences and Antiquity of the Early Rock Art of Western Arnhem Land*. Unpublished PhD Thesis. The Australian National University, Canberra Australia.
- Jones, T., et al., 2017. Radiocarbon age constraints for a Pleistocene–Holocene transition rock art style: the Northern Running figures of the east Alligator River region, western Arnhem Land, Australia. *J. Archaeol. Sci.: Reports* 11, 80–89. <https://doi.org/10.1016/j.jasrep.2016.11.016>.
- Jones, T., et al., 2020. Rethinking the age and unity of large naturalistic animal forms in early Western Arnhem Land Rock Art, Australia. *Aust. Archaeol.* <https://doi.org/10.1080/03122417.2020.1826080>.
- Jones, R., Johnson, L., 1985. Deaf Adder Gorge: Lindner Site, Nauwalabila. In: Jones, Rhys (Ed.), *Archaeological Research in Kakadu National Park, Special Publication 13*. Australian National Parks and Wildlife Service, pp. 165–227.
- Kemp, C.W., Tibby, J., Arnold, L.J., Barr, C., 2019. Australian hydroclimate during Marine Isotope Stage 3: a synthesis and review. *Quat. Sci. Rev.* 204, 94–104. <https://doi.org/10.1016/j.quascirev.2018.11.016>.
- Chippindale, C., Tacon, P.S.C., 1998. In: Steinbring, J., Watchman, A., Faulstich, P., Tacon, P.S.C. (Eds.), *Time and Space: Dating and Spatial Considerations in Rock Art Research: Papers of Symposia F and E, Second AURA Congress, Cairns 1992*. Australian Rock Art Research Association.
- Koch, H., 1997. Comparative linguistics and Australian prehistory. In: Patrick, McConvell, Nicholas, Evans (Eds.), *Archaeology and linguistics: Aboriginal Australia in global perspective*. Oxford University Press, Melbourne, pp. 27–43.
- Kuijjer, E., Haigh, I., Marsh, R., Farr, H., 2022. Changing tidal dynamics and the role of the marine environment in the maritime migration to Sahul: special issue: the impact of upper pleistocene climatic and environmental change on hominin occupations and landscape use. *PaleoAnthropology (Part 1)*, 134–148. <https://doi.org/10.48738/2022.iss1.105>.
- Lambeck, K., Chappell, J., 2001. Sea level change through the last glacial cycle. *Science* 292, 679–686. <https://doi.org/10.1126/science.1059549>.
- Lambeck, K., Rouby, H., Purcell, A., Sun, Y., Sambridge, M., 2014. Sea level and global ice volumes from the last glacial maximum to the Holocene. *Proc. Natl. Acad. Sci. USA* 111, 15296–15303. <https://doi.org/10.1073/pnas.1411762111>.
- Leach, J., et al., 2021. The integrated cultural landscape of North Gidley Island: coastal, intertidal and nearshore archaeology in Murujuga (Dampier Archipelago), Western Australia. *Aust. Archaeol.* 87, 251–267. <https://doi.org/10.1080/03122417.2021.1949085>.
- Lewis, D., 1988. *The Rock Paintings of Arnhem Land, Australia: Social, Ecological and Material Culture Change in the Post-glacial Period*. BAR Publishing, Oxford.
- Lewis, D., 1997. Bradshaws: the view from Arnhem land. *Aust. Archaeol.* 44, 1–16.
- Lewis, S.E., Sloss, C.R., Murray-Wallace, C.V., Woodroffe, C.D., Smithers, S.G., 2013. Post-glacial sea-level changes around the Australian margin: a review. *Quat. Sci. Rev.* 74, 115–138. <https://doi.org/10.1016/j.quascirev.2012.09.006>.
- Lin, Y., et al., 2021. A reconciled solution of Meltwater Pulse 1A sources using sea-level fingerprinting. *Nat. Commun.* 12, 2015. <https://doi.org/10.1038/s41467-021-21990-y>.
- López, P., et al., 2016. Terrestrial and maritime taphonomy: differential effects on spatial distribution of a Late Pleistocene continental drowned faunal bone assemblage from the Pacific coast of Chile. *Archaeological and Anthropological Sci* 8, 277–290. <https://doi.org/10.1007/s12520-015-0275-y>.
- Lorenz, D.J., Nieto-Lugilde, D., Blois, J.L., Fitzpatrick, M.C., Williams, J.W., 2016. Downscaled and debiased climate simulations for North America from 21,000 years ago to 2100 AD. *Sci. Data* 3, 1–19. <https://doi.org/10.1038/sdata.2016.48>.
- Maloney, T., O'Connor, S., Wood, R., Aplin, K., Balme, 2018. J. Carpenters Gap 1: a 47,000 year old record of indigenous adaption and innovation. *Quat. Sci. Rev.* 191, 204–228. <https://doi.org/10.1016/j.quascirev.2018.05.016>.
- Marx, S.K., et al., 2021. Monsoon driven ecosystem and landscape change in the 'Top End' of Australia during the past 35 kyr. *Palaeogeogr. Palaeoclimatol. Palaeoecol.* 583, 110659. <https://doi.org/10.1016/j.palaeo.2021.110659>.
- May, S.K., Johnston, I., Taçon, P., Domingo Sanz, I., Goldhahn, J., 2018. Early Australian anthropomorphs: Jabiluka's dynamic figure rock paintings. *Camb. Archaeol. J.* 28, 67–83. <https://doi.org/10.1017/S095977431700052X>.
- McCarthy, J., et al., 2022. Beneath the Top End: a regional assessment of submerged archaeological potential in the Northern Territory, Australia. *Aust. Archaeol.* 88, 65–83. <https://doi.org/10.1080/03122417.2021.1960248>.
- Neal, R., Stock, E., 1986. Pleistocene occupation in the south-east Queensland coastal region. *Nature* 323, 618–621. <https://doi.org/10.1038/323618a0>.
- Norman, K., O'Connor, S., Bird, M., 2021. In: McNiven, Ian J., Bruno, David (Eds.), *The Oxford Handbook of the Archaeology of Indigenous Australia and New Guinea*. Oxford University Press, Oxford, pp. 215–240. <https://doi.org/10.1093/oxfordhb/9780190095611.013.8>.
- Norman, K., et al., 2018. An early colonisation pathway into northwest Australia 70–60,000 years ago. *Quat. Sci. Rev.* 180, 229–239. <https://doi.org/10.1016/j.quascirev.2017.11.023>.
- Norman, K., et al., 2022. Human occupation of the Kimberley coast of northwest Australia 50,000 years ago. *Quat. Sci. Rev.* 288, 107577. <https://doi.org/10.1016/j.quascirev.2022.107577>.
- O'Connor, S., 1999. *30,000 Years of Aboriginal Occupation: Kimberley, North West Australia*. Terra Australis, 14. Research School of Pacific and Asian Studies, The Australian National University, Canberra.
- O'Leary, M.J., Paumard, V., Ward, I., 2020. Exploring Sea Country through high-resolution 3D seismic imaging of Australia's NW shelf: resolving early coastal landscapes and preservation of underwater cultural heritage. *Quat. Sci. Rev.* 239, 106353. <https://doi.org/10.1016/j.quascirev.2020.106353>.
- Roberts, R.G., et al., 1994. The human colonisation of Australia: optical dates of 53,000 and 60,000 years bracket human arrival at Deaf Adder Gorge, Northern Territory. *Quat. Sci. Rev.* 13, 575–583. [https://doi.org/10.1016/0277-3791\(94\)90080-9](https://doi.org/10.1016/0277-3791(94)90080-9).
- Rowe, C., et al., 2021. Vegetation over the last glacial maximum at Girraween Lagoon, monsoonal northern Australia. *Quat. Res.* 102, 39–52. <https://doi.org/10.1017/qua.2020.50>.
- Solihuddin, T., Bufarale, G., Blakeway, D., O'leary, M.J., 2016. Geomorphology and late Holocene accretion history of Adele Reef: a northwest Australian mid-shelf platform reef. *Geo Mar. Lett.* 36, 465–477. <https://doi.org/10.1017/qua.2010.50>.
- Stuiver, M., Reimer, P.J., 1993. Extended ¹⁴C data base and revised CALIB 3.0 ¹⁴C age calibration program. *Radiocarbon* 35, 215–230. <https://doi.org/10.1017/S0033822200013904>.
- Sturt, F., Flemming, N., Carabias, D., Jöns, H., Adams, J., 2018. The next frontiers in research on submerged prehistoric sites and landscapes on the continental shelf. *Proc. Geologists' Assoc.* 129, 654–683. <https://doi.org/10.1016/j.pgeola.2018.04.008>.
- Tacon, P., Chippindale, C., 1994. Australia's ancient warriors: changing depictions of fighting in the rock art of Arnhem Land. *NT. Camb. Archaeol. J.* 4, 211–248. <https://doi.org/10.1017/S0959774300001086>.
- Taçon, P.S., et al., 2020. Maliwawa figures—a previously undescribed Arnhem Land rock art style. *Aust. Archaeol.* 86, 208–225.
- Tallavaara, M., Eronen, J.T., Luoto, M., 2018. Productivity, biodiversity, and pathogens influence the global hunter-gatherer population density. *Proc. Natl. Acad. Sci. USA* 115, 1232–1237.
- Timmermann, A., Friedrich, T., 2016. Late Pleistocene climate drivers of early human migration. *Nature* 538, 92–95.
- Tizzard, L., Bicket, A., Benjamin, J., Loecker, D.D., 2014. A Middle Palaeolithic site in the southern North Sea: investigating the archaeology and palaeogeography of Area 240. *J. Quat. Sci.* 29, 698–710.
- van Andel, T.H., Heath, G.R., Moore, T., McGeary, D.F., 1967. Late Quaternary history, climate, and oceanography of the Timor Sea, northwestern Australia. *Am. J. Sci.* 265, 737–758.
- Veth, P., et al., 2017. Early human occupation of a maritime desert, Barrow Island, North-West Australia. *Quat. Sci. Rev.* 168, 19–29. <https://doi.org/10.1016/j.quascirev.2017.05.002>.
- Veth, P., Myers, C., Heaney, P., Ouzman, S., 2018. Plants before farming: the deep history of plant-use and representation in the rock art of Australia's Kimberley region. *Quat. Int.* 489, 26–45. <https://doi.org/10.1016/j.quaint.2016.08.036>.
- Veth, P., et al., 2019. Minjiwarra: archaeological evidence of human occupation of Australia's northern Kimberley by 50,000 BP. *Aust. Archaeol.* 85, 115–125. <https://doi.org/10.1080/03122417.2019.1650479>.
- Veth, P., et al., 2020. A strategy for assessing continuity in terrestrial and maritime landscapes from Murujuga (Dampier Archipelago), North West Shelf, Australia. *J. Int. Coast Archaeol.* 15, 477–503.
- Walsh, G.L., 1994. *Bradshaws: Ancient Rock Paintings of North-West Australia*. The Bradshaw Foundation, Geneva.
- Walsh, G.L., 2000. *Bradshaw Art of the Kimberley*. Takarakka Nowan Kas Publications, Toowoong, Qld.

- Ward, I.A.K., et al., 2005. Late Quaternary landscape evolution in the Keep River region, northwestern Australia. *Quat. Sci. Rev.* 24, 1906–1922. <https://doi.org/10.1016/j.quascirev.2004.11.004>.
- Ward, I.A.K., et al., 2006. Comparison of sedimentation and occupation histories inside and outside rock shelters, Keep-River region, northwestern Australia. *Geoarchaeology* 21, 1–27. <https://doi.org/10.1002/geo.20087>.
- Ward, I., Larcombe, P., Veth, P., 2015. A new model for coastal resource productivity and sea-level change: the role of physical sedimentary processes in assessing the archaeological potential of submerged landscapes from the northwest Australian continental shelf. *Geoarchaeology* 30, 19–31.
- Werz, B.E., Flemming, N.C., 2001. Discovery in Table Bay of the oldest handaxes yet found underwater demonstrates preservation of hominid artefacts on the continental shelf. *South Afr. J. Sci.* 97, 183–185.
- Wilby, R.L., Wigley, T.M., 1997. Downscaling general circulation model output: a review of methods and limitations. *Prog. Phys. Geogr.* 21, 530–548.
- Williams, A.N., 2013. A new population curve for prehistoric Australia. *Proceedings of the Royal Society B* 280, 20130486. <https://doi.org/10.1098/rspb.2013.0486>.
- Williams, A.N., Ulm, S., Cook, A.R., Langley, M.C., Collard, M., 2013. Human refugia in Australia during the Last Glacial Maximum and terminal Pleistocene: a geospatial analysis of the 25–12 ka Australian archaeological record. *J. Archaeol. Sci.* 40, 4612–4625.
- Williams, A.N., Ulm, S., Sapienza, T., Lewis, S., Turney, C.S., 2018. Sea-level change and demography during the last glacial termination and early Holocene across the Australian continent. *Quat. Sci. Rev.* 182, 144–154.
- Wiseman, C., et al., 2021. A multi-scalar approach to marine survey and underwater archaeological site prospection in Murujuga, Western Australia. *Quat. Int.* 584, 152–170.
- Wood, R., et al., 2016. Towards an accurate and precise chronology for the colonization of Australia: the example of Riwí, Kimberley, Western Australia. *PLoS One* 11, e0160123. <https://doi.org/10.1371/journal.pone.0160123>.
- Woodroffe, C., Chappell, J., Thom, B., 1986. *Geomorphological Dynamics and Evolution of the South Alligator Tidal River and Plains, Northern Territory*. The Australian National University, Canberra.
- Yokoyama, Y., Lambeck, K., De Deckker, P., Johnston, P., Fifield, L.K., 2000. Timing of the Last Glacial Maximum from observed sea-level minima. *Nature* 406, 713–716.
- Yokoyama, Y., De Deckker, P., Lambeck, K., Johnston, P., Fifield, L., 2001a. Sea-level at the Last Glacial Maximum: evidence from northwestern Australia to constrain ice volumes for oxygen isotope stage 2. *Palaeogeogr. Palaeoclimatol. Palaeoecol.* 165, 281–297.
- Yokoyama, Y., Purcell, A., Lambeck, K., Johnston, P., 2001b. Shore-line reconstruction around Australia during the last glacial maximum and late glacial stage. *Quat. Int.* 83–85, 9–18.
- Grøn, O., Skaarup, J., 2004. Submerged Stone Age Coastal Zones in Denmark: investigation strategies and results. In: Flemming, N.C. (Ed.), *Man and Sea in the Mesolithic*. English Heritage, pp. 53–56.